

Lift Disturbance Cancellation with Rapid-Flap Actuation

Albert Medina^{*1}, Maziar S. Hemati^{†2}, and Matthew Rockwood^{‡1}

¹*Air Force Research Laboratory, Wright-Patterson AFB, OH, 45433*

²*University of Minnesota, Twin Cities, Minneapolis, MN 55455*

Experimental results examining a rapidly-deflecting simple flap of a wall-to-wall NACA 0006 wing in a water tunnel at $Re = 40k$ are presented for a survey of flap deflections designed to negate the lift-transient from an imposed plunge motion of the entire wing. The plunge, over a period ranging from eight convective times to one convective time, is regarded as a vertical disturbance, or a “gust”. The flap deflection history is initially derived from Theodorsen’s formula for unsteady flap motions, from which one obtains phase and amplitude information. The theoretical derivation makes the standard assumptions of attached flow, planar wake, and no leading edge vortices. Experimental data measurements of lift on the fore-element and the flap of the wing are examined for pure-plunge, for pure flap deflection, and for the combined airfoil plunge and flap deflection motion. The latter shows up to 87% of lift cancellation, verifying the limited, but substantial applicability of Theodorsen’s formula. Improvements over the theoretical formulation of lift cancellation are sought by constructing empirical models for both airfoil plunge and flap deflection. The empirical models for airfoil plunge and flap deflection are constructed independent of one another and their superposition is employed to approximate the total lift in combined plunge and deflection motions. It is shown that although the empirical model approach performs similar to the inviscid theory of Theodorsen’s model, the empirical model proves more effective in suppressing the leading-edge vortex induced in plunge.

Nomenclature

α_{LE}	=	leading-element angle of attack
α_{eff}	=	effective angle of attack
c	=	chord length
b	=	semi-chord length
U_∞	=	freestream speed
Re	=	Reynolds number, cU_∞/ν
k	=	reduced frequency
h	=	plunge position
δ	=	flap deflection angle
ϕ	=	flap-deflection phase lead
C_L	=	lift coefficient
C_k	=	Theodorsen function
\tilde{x}	=	internal state of the system
θ	=	state-space model input
y	=	state-space model output

*Research Scientist, Aerodynamic Technology Branch, Aerospace Vehicles Division, Aerospace Systems Directorate. AIAA Senior Member

†Assistant Professor, Department of Aerospace Engineering and Mechanics. AIAA Senior Member.

‡Research Scientist, AS&M, Aerodynamic Technology Branch, Aerospace Vehicles Division, Aerospace Systems Directorate. AIAA Member.

I. Introduction

RECENT parameter studies on transient deflection of fast flaps have shown that immediately upon deflection of the flap, even in a separated flow (the main element being at 20° incidence), there will be a lift-response in some proportion to the flap deflection-rate [1]. A simplified analytic model for lift coefficient history, composed of (1) added-mass [2], (2) pitch-rate or virtual camber, and (3) quasi-steady lift from airfoil theory, was moderately successful for transient lift response, but ignored wake-effects. The wake effects can be recovered for sinusoidal motions using Theodorsen’s formula for a flapped airfoil, an example of which can be seen in the presentation by Jaworski [3]. It was found that as flap deflection rate increased, not only was the inviscid solution for lift recovered (alternatively, the penalty of flow separation was attenuated), but there was an entrainment effect over the suction side of the fore-element and the flap, such that the mean of the lift hysteresis loop was well above both the corresponding measured static value and the nominal inviscid static value. An offset, depending on flap motion rate and initial position, was proposed.

In the present work, Theodorsen’s formula is again utilized, but with the wing fore-element at zero incidence, and the flap oscillating about zero incidence angle. Thus the mean lift is a zero mean, regardless of flap motion rate. A spatially-uniform “disturbance” is introduced by imposing a sinusoidal plunge-motion on the entire wing (the fore-element and the flap). This may lead to flow separation, depending on the effective plunge-induced angle of attack, or alternatively on the plunge frequency. The flap is deflected at the same frequency as the plunge, also sinusoidally, in an attempt to cancel the lift disturbance from plunge. Because the flap frequency and plunge frequency are locked, there is no opportunity to exploit high-lift transients from faster flap deflection [1]. In this study a parameter sweep of the disturbance frequency and amplitude is investigated, and the lift cancellation is informed by both Theodorsen’s formula, and an empirical state-space model.

The method of McGowan et al. [4] was pursued in recourse to Theodorsen’s formula to seek “lift equivalence”. Plunge-flap lift-cancellation in the experiment was contingent on the validity of Theodorsen’s formula, but this was shown to be remarkably robust, even in separated flow. For now, no advocacy position on whether Theodorsen’s formula is superior or deficient is taken, it is simply used as a rubric for connecting a plunge motion with a desired flap motion. Better theoretical or phenomenological treatments doubtlessly exist. Instead, the aim is to find at least an approximately suitable model for the “plant” (aerodynamic response of the flap) and the “disturbance” (the plunge), for what will eventually be a feed-forward control system, relying on negation of the flap model; this would follow Kerstens et al. [5]. This study considers only the prescriptive (deterministic) motion of the flap.

As in prior work, the theme remains control of flow separation on a wing undergoing unsteady motion, where it is unacceptable to endure a lag of several convective-times between control-initiation and aerodynamic response [6] (one convective time is $tU_\infty/c = 1$, where c is the airfoil chord, and U_∞ the freestream speed). Rennie and Jumper [7] examined slower flap responses (in the context of the present experiment), found no apparent lag in response, and that deleterious effects of flow separation, which were measured in a static survey of flap incidence, were attenuated during dynamic flap deflection [8]. This is in contrast to the usual case for pointwise (fluidic or electric) flow control, where for several convective times upon initiation of actuation, there is a deadband in response or a negative response in lift [9].

II. Experimental Setup

Experiments were performed in the U.S. Air Force Research Laboratory (AFRL) Horizontal Free-Surface Water Tunnel, depicted in Fig. 1,(left). The tunnel has a 4:1 contraction and 46 cm wide by 61 cm high test section with a freestream speed range of 3-105 cm/s and a streamwise turbulence intensity of $\sim 1.0\%$ for speeds between 7-80 cm/s. The tunnel is fitted with a three-degree-of-freedom motion stage, consisting of a triplet of H2W Technologies linear motors, driven by AMC DigiFlex servo drives interfaced with a Galil DMC 4040 four-axes motion controller with user-selected proportional-integral-derivative gain constants for each axis. A plastic 3-D printed NACA 0006 airfoil of 20 cm chord (physical aspect ratio of 2.25), strengthened by spanwise carbon-fiber rods, is bisected about the mid-chord position as illustrated in Fig. 1,(right). The test article spans the test section with a nominal 1mm gap at each wingtip. The fore element is rigidly connected to the plunge rod of the upstream vertical linear motor. The resulting aft element, or flap, is analogously connected to the downstream vertical linear motor, but is constrained by a linkage mechanism to the fore element such that the relative motion between the two vertical motors results in a pitching motion of the

flap. The gap between the two elements measures 0.5 mm and is bridged with a flexible rubber film of 0.2 mm thickness to prevent flare-up. The flap incidence angle is limited to $\pm 45^\circ$ with respect to the horizontal plane. The fore element fixed-incidence angle is $\alpha_{LE} = 0^\circ$, corresponding to an attached flow with zero net lift. Experiments are performed at Reynolds number $Re = 40k$.

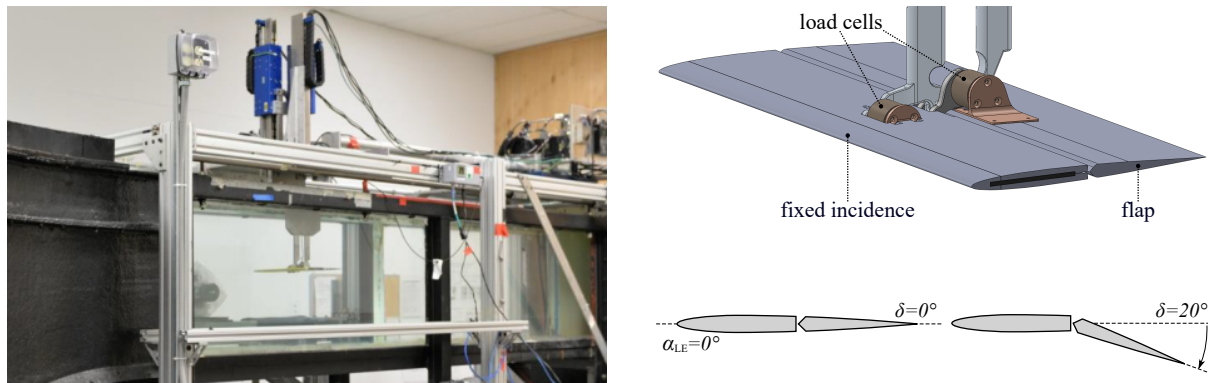


Figure 1. (left) Water tunnel facility. (right) NACA0006 configuration and angular definitions.

Force measurement was conducted via two ATI NANO-25 IP68 six-component force balances. Each airfoil element was supplied a dedicated force balance affixed to its respective frame. Importantly, there is no mechanical connection between the fore and aft elements; the forces measured for each element were therefore measured independently. Measurements were sampled at a rate of 1 kHz and treated by a second-order Butterworth low-pass filter with a cutoff frequency of 8 Hz. For periodic motions, the flap motion and the wing-plunge continue for 70 periods. The first few periods evince effects of start-up transients; therefore the first 10 periods are discarded for the purpose of phase-averaging. Likewise, the last 10 periods are also discarded. Force histories were constructed from phase averaging over the remaining fifty consecutive periods of motion. Static forces were derived from time-averaging over a hold period of 10s for each flap deflection angle. Lift coefficient was non-dimensionalized as $C_L = (L/0.5\rho U_\infty^2 S)$, where L is the measured lift, ρ is the fluid density, U_∞ is the freestream speed, S is the planform area, and c is the total chord length. Planar flow visualization was performed at the three-quarter span-wise position. Rhodamine-590 was introduced at the leading edge and the trailing edge of the airfoil and fluoresced by an Nd:YLF laser sheet (Photonics Industries DM50-527, 55 mJ/pulse, 10 kHz max). To minimize surface reflections the camera was outfitted with an optical filter (Tiffen, Orange 21) compatible with the fluorescence emission.

The kinematic schedules of airfoil plunge and flap deflection are respectively expressed in Eq. (1):

$$h = h_0 e^{i\omega t} \quad \delta = \delta_0 e^{i(\omega t + \phi)} = \delta_0 e^{i\omega t} e^{i\phi} \quad (1)$$

where ω is the angular frequency, h is the wing plunge history, and h_0 is the plunge amplitude. Analogously, the flap deflection motion was a sinusoid of amplitude δ_0 and with a phase lead angle of ϕ over the plunge cycle. The plunge motion was employed as a kinematic-driven gust which provided a spatially-uniform temporally-variant vertical velocity component. The lift coefficient was approximated as linearly time-invariant and is expressed as the summation of airfoil plunge and flap deflection contributions given by Eq. (2) as:

$$C_L = C_{L,\text{plunge}} + C_{L,\text{defl.}} \quad (2)$$

where the subscripts denote the respective contributions of airfoil plunge and flap deflection to lift coefficient. Note the exclusion of a steady state incidence term in Eq. (2), as the baseline situation (no plunge and no flap deflection) has zero lift.

III. Theory

A. Theodorsen Modeling

Following Jaworski's treatment of Theodorsen's model [3] the respective lift contributions of airfoil plunge and flap deflection may be expressed as:

$$C_{L,\text{plunge}} = \pi\rho b^2\ddot{h} + 2\pi\rho U_\infty b C_k \dot{h} \quad (3)$$

and

$$C_{L,\text{defl.}} = \pi\rho b^2 \left[\frac{1}{2} U_\infty \dot{\delta} + \frac{2}{3\pi} b \ddot{\delta} \right] + 2\pi\rho U_\infty b C_k \left[\frac{2+\pi}{2\pi} U_\infty \delta + \frac{4+\pi}{4\pi} b \dot{\delta} \right] \quad (4)$$

where ρ is the fluid density, b is the semi-chord length ($c/2$), U_∞ is the freestream speed, and C_k is the Theodorsen function ($C_k = F(k) + iG(k)$) for reduced frequency $k = \omega b/U_\infty$. Eqs. (3) and (4) were derived using a small-angle approximation, assumed a planar wake, and were formulated for an attached flow.

Following McGowan et al. [4], cancellation of lift from airfoil plunge by lift from flap deflection is achieved by setting Eq. (2) to zero:

$$C_{L,\text{plunge}} = -C_{L,\text{defl.}} \quad (5)$$

Although the lift response is modeled separately for plunge and deflection, a key assumption is that the linear superposition of the two components is valid. To derive an analytical expression for flap deflection amplitude and phase necessary for the cancellation of plunge effects, the kinematic schedules of Eq. (1) for h and δ and their respective derivatives are substituted into Eqs. (3) and (4). The resulting complex lift coefficient expressions are then substituted into the zero-lift criterion of Eq (5), where the real portion of the final expression yields Eq. (6):

$$\begin{aligned} [\pi\rho b^2\omega^2 + 2\pi\rho U_\infty b G\omega] h_0 = & \\ & \left[\left(-\frac{\pi}{2}\rho b^2 U_\infty - (2+\pi)\rho U_\infty b G - \frac{4+\pi}{2}\rho U_\infty b^2 \omega F \right) \sin\phi \right. \\ & \left. + \left(-\frac{2}{3}\rho b^3 \omega^2 + (2+\pi)\rho U_\infty^2 b F - \frac{4+\pi}{2}\rho U_\infty b^2 \omega G \right) \cos\phi \right] \delta_0 \end{aligned} \quad (6)$$

or

$$[A_1] h_0 = [A_2 \sin\phi + A_3 \cos\phi] \delta_0 \quad (7)$$

And the imaginary portion yields Eq. (8):

$$\begin{aligned} [-2\pi\rho U_\infty b \omega F] h_0 = & \\ & \left[\left(-\frac{2}{3}\rho b^3 \omega^2 + (2+\pi)\rho U_\infty^2 b F - \frac{4+\pi}{2}\rho U_\infty b^2 \omega G \right) \sin\phi \right. \\ & \left. + \left(\frac{\pi}{2}\rho U_\infty b^2 \omega + (2+\pi)\rho U_\infty^2 b G + \frac{4+\pi}{2}\rho U_\infty b^2 \omega F \right) \cos\phi \right] \delta_0 \end{aligned} \quad (8)$$

or

$$[B_1] h_0 = [B_2 \sin\phi + B_3 \cos\phi] \delta_0 \quad (9)$$

Division of Eq. (6) by Eq. (8) eliminates the dependency on plunge and flap deflection amplitudes. Further division of the numerator and denominator by $\cos\phi$ produces an expression for pitch phase lead:

$$\phi = \tan^{-1} \left(\frac{B_1 A_3 - A_1 B_3}{A_1 B_2 - B_1 A_2} \right) \quad (10)$$

The procedure undertaken in this work first prescribes a flap deflection amplitude and reduced frequency, k . Then using Eq (10) the corresponding phase lead, ϕ , is calculated. The phase lead is then substituted into

either Eq. (6) or (8) to determine the ratio of plunge amplitude to flap deflection amplitude, h_0/δ_0 . When these calculated kinematic parameters are executed in experiments the theoretical result is an identically zero lift coefficient history. The Theodorsen approach is employed in examining the gust mitigation capabilities of flap amplitudes of $\delta_0 = 10^\circ$ and 20° for reduced frequencies $k = [0.3989, 0.7979, 1.5959, 3.1919]$. Such operational frequencies invoke a highly unsteady flow field. Cases to be examined within the Theoretical framework of Theodorsen's model are summarized in Table 1.

Table 1. Theodorsen Model Motion Parameters

	Motion	h_0/b	ϕ [deg]
Case 1: $k = 0.3989, \delta_0 = 10^\circ$	pitch+plunge	-0.3791	81.41
	pure pitch	0	0
	pure plunge	-0.3791	0
Case 2: $k = 0.7979, \delta_0 = 10^\circ$	pitch+plunge	-0.1985	77.99
	pure pitch	0	0
	pure plunge	-0.1985	0
Case 3: $k = 1.5959, \delta_0 = 10^\circ$	pitch+plunge	-0.1028	69.52
	pure pitch	0	0
	pure plunge	-0.1028	0
Case 4: $k = 3.1919, \delta_0 = 10^\circ$	pitch+plunge	-0.0596	52.45
	pure pitch	0	0
	pure plunge	-0.0596	0
Case 5: $k = 0.7979, \delta_0 = 20^\circ$	pitch+plunge	-0.3971	77.99
	pure pitch	0	0
	pure plunge	-0.3971	0
Case 6: $k = 1.5959, \delta_0 = 20^\circ$	pitch+plunge	-0.2057	69.52
	pure pitch	0	0
	pure plunge	-0.2057	0

B. Empirical State-Space Modeling

In this section, the approach used to extract a state-space model from an empirical sequence of input-output data is detailed. This model was pursued in an attempt to improve upon the results of the theoretical Theodorsen model. The model input is denoted as $\ddot{\theta}$, which corresponded to $\ddot{\delta}$ for flap modeling and \ddot{h} for plunge modeling. The output for each model was the lift coefficient minus the lift at the initial set point $y = C_L - C_{L_0}$. In order to compare directly with the Theodorsen models of the previous section, the discrete-time models were later converted to continuous-time realizations using a Tustin transformation [10].

Specifically, a system of the form,

$$\begin{bmatrix} \tilde{x}_{k+1} \\ \theta_{k+1} \\ \dot{\theta}_{k+1} \end{bmatrix} = \begin{bmatrix} \tilde{A} & B_\theta & B_\delta \\ 0 & 1 & \Delta t \\ 0 & 0 & 1 \end{bmatrix} \begin{bmatrix} \tilde{x}_k \\ \theta_k \\ \dot{\theta}_k \end{bmatrix} + \begin{bmatrix} B_{\ddot{\theta}} \\ \Delta t^2/2 \\ \Delta t \end{bmatrix} \ddot{\theta}_k \quad (11a)$$

$$y_k = \begin{bmatrix} \tilde{C} & C_{L_\theta} & C_{L_\delta} \end{bmatrix} \begin{bmatrix} \tilde{x}_k \\ \theta_k \\ \dot{\theta}_k \end{bmatrix} + C_{L_{\ddot{\theta}}} \ddot{\theta}_k \quad (11b)$$

was developed, where prior knowledge of the kinematic relation from $\ddot{\delta}$ to $\{\delta, \dot{\delta}\}$ was leveraged. The internal state of the system $\tilde{x} \in \mathbb{R}^n$ captured transient aerodynamic effects. Following the approach in [11], the equations of motion were written to a form that was conducive to solving for the unknown dynamics using standard methods. Specifically, known kinematic quantities were treated as inputs for the purposes of system

identification, i.e. $u_k = (\ddot{\theta}_k, \dot{\theta}_k, \theta_k)$, and worked with the linear time-invariant (LTI) system in the form,

$$\tilde{x}_{k+1} = \tilde{A}\tilde{x}_k + \underbrace{\begin{bmatrix} B_{\ddot{\theta}} & B_{\dot{\theta}} & B_{\theta} \end{bmatrix}}_{\tilde{B}} u_k \quad (12a)$$

$$y_k = \tilde{C}\tilde{x}_k + \underbrace{\begin{bmatrix} C_{L_{\ddot{\theta}}} & C_{L_{\dot{\theta}}} & C_{L_{\theta}} \end{bmatrix}}_{\tilde{D}} u_k \quad (12b)$$

Given a sequence of input-output data $\{u_k, y_k\}$, the unknown system matrices $(\tilde{A}, \tilde{B}, \tilde{C}, \tilde{D})$ were then determined by means of various subspace techniques for solving the so-called ‘‘combined deterministic-stochastic problem’’ [12].

The flap-deflection and wing-plunge models were constructed independently by respective pure-deflection and pure-plunge motions provided by a smoothed ramp fitted to a sinusoid profile of reduced frequency $k = 1.59$. The speed of motion amounted to a smoothed step-change. The flap was deflected from an initial incidence of $\delta = 0^\circ$ and concluded at $\delta = 20^\circ$ in a pitch-hold maneuver. The wing was plunged a depth of $h/b = 0.6$. During plunge the wing remains non-deflected. Reconstructed lift histories are compared with guiding experimental measurements in Fig. 2. The dimension of the internal state $\tilde{x}(t)$ was varied from $n = 1$ to $n = 3$. For pure deflection, $n = 1$ was selected to model the lift response, as it had the best qualitative agreement with the initial transient before relaxation. Higher-order models exhibited oscillatory modes. In pure plunge, $n = 2$ was selected to model the lift response, as this was found to capture the force history most accurately.

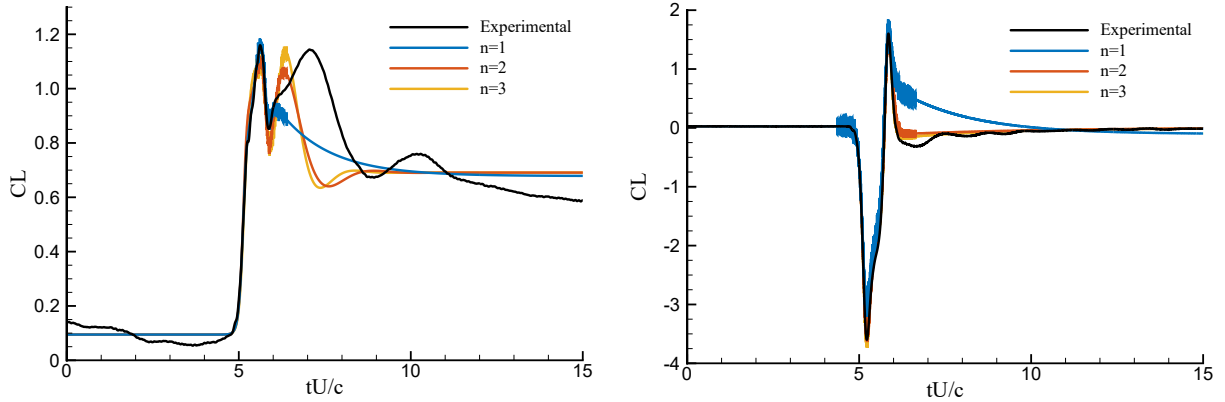


Figure 2. Indicial response reconstruction: (left) pure flap deflection, (right) pure wing plunge.

The frequency response of the modeled transfer functions for flap deflection, $G_{\text{defl.}}(s) = \mathcal{L}[C_L]/\mathcal{L}[\ddot{\delta}]$, and plunge, $G_{\text{plunge}}(s) = \mathcal{L}[C_L]/\mathcal{L}[\ddot{h}]$, are shown in Fig. 3. The input motion is $\ddot{\delta}$ for pure deflection and \ddot{h} for pure wing plunge. The output is lift coefficient. The procedure to determine the theoretical deflection amplitude and phase lead required to cancel the lift generated by a given plunge is as follows. Ideally, the lift response of the airfoil would be linearly dependent on flap and plunge motions, allowing for the respective contributions to be superimposed for cancellation, as in Eq. (5). The linear approximation yields an expression for plunge and flap deflection magnitude:

$$\|G_{\text{plunge}}\| \|\ddot{h}\| + C_{L_{o,\text{plunge}}} = \|G_{\text{defl.}}\| \|\ddot{\delta}\| + C_{L_{o,\text{defl.}}} \quad (13)$$

If flap acceleration is used as an input to the model, the plunge acceleration can be determined as:

$$\|\ddot{h}\| = \frac{\left(\|G_{\text{defl.}}\| \|\ddot{\delta}\| + C_{L_{o,\text{defl.}}} - C_{L_{o,\text{plunge}}} \right)}{\|G_{\text{plunge}}\|} \quad (14)$$

Alternatively, if plunge acceleration is the input, flap acceleration can be determined using the following expression:

$$\|\ddot{\delta}\| = \frac{\left(\|G_{\text{plunge}}\| \|\ddot{h}\| + C_{L_o,\text{plunge}} - C_{L_o,\text{defl.}}\right)}{\|G_{\text{defl.}}\|}. \quad (15)$$

The cancellation of lift between airfoil plunging and flap deflection motions requires the lift generated by the two motions to be 180° out of phase with one another. The phase of the lift generated by plunge is equal to the plunge input phase, $\angle\ddot{h}$, plus the output phase shift in the model, $\angle G_{\text{plunge}}$. A similar relationship exists for flap deflection, yielding the following equation:

$$\angle\ddot{h} + \angle G_{\text{plunge}} = \angle\ddot{\delta} + \angle G_{\text{defl.}} + \pi. \quad (16)$$

Therefore, the required phase lead, ϕ , between the airfoil plunge and flap deflection needed to obtain zero lift throughout the motion is determined as:

$$\phi = \angle\ddot{h} - \angle\ddot{\delta} = \angle G_{\text{defl.}} - \angle G_{\text{plunge}} + \pi. \quad (17)$$

where the required phase and magnitude values for a given reduced frequency of operation are populated from the frequency response data of Fig. 3.

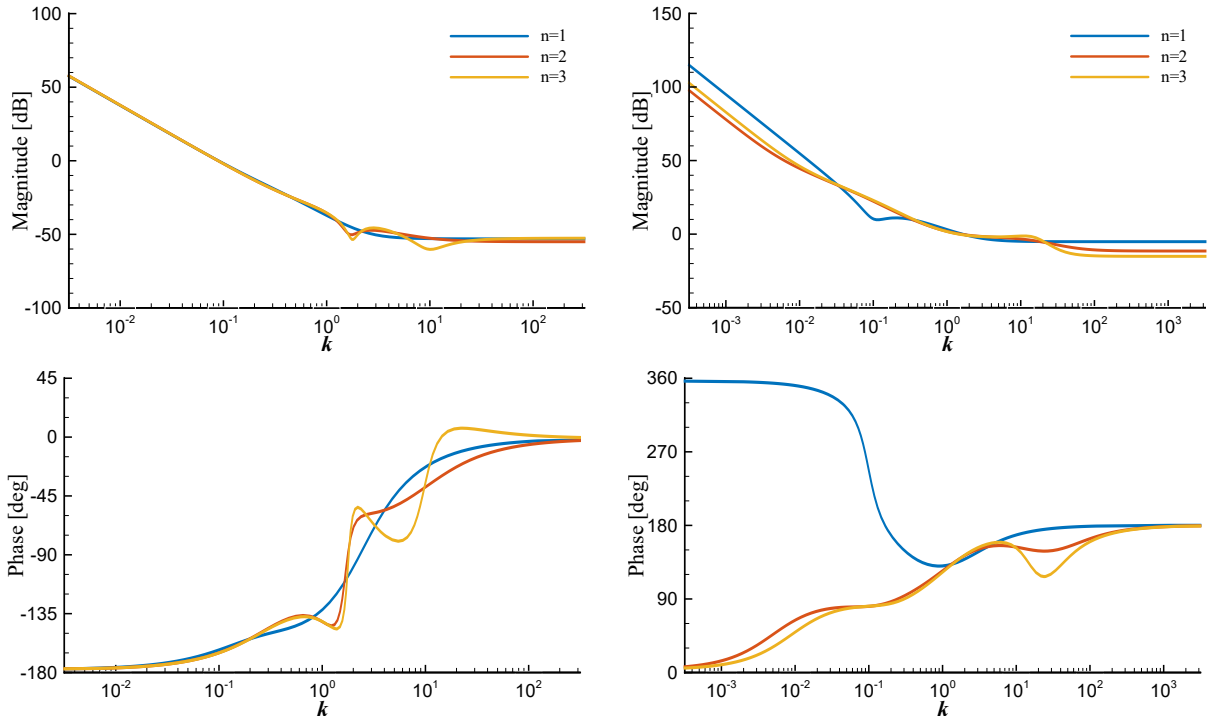


Figure 3. Frequency response of transfer functions. Columns: (*left*) pure flap deflection, (*right*) pure wing plunge.

Cases that were examined within the state-space framework of the empirical model are summarized in Table 2.

Table 2. Empirical Model Motion Parameters

	Motion	h_0/b	ϕ [deg]
Case 7: $k = 1.5959$, $\delta_0 = 20^\circ$	pitch+plunge	0.1565	70.41
	pure pitch	0	0
	pure plunge	0.1565	0
Case 8: $k = 1.5959$, $\delta_0 = 27.63^\circ$	pitch+plunge	0.2057	70.41
	pure pitch	0	0
	pure plunge	0.2057	0

IV. Results and Discussion

Direct force measurements and dye visualization were used to gauge the effectiveness of flap deflection in mitigating the influence of temporal variations in the relative vertical velocity component imposed by airfoil plunge. Prior to examining the role of dynamic deflection (or plunge) the static lift response is presented to provide insight into the state of separation experienced over the flap. Results for static lift in response to flap deflection are shown in Fig. 4. As previously noted, the static survey is performed by a slow jog in deflection followed by a hold period. To demonstrate a steady state is achieved in this approach, static lift was measured for a deflection schedule of $\delta = 0^\circ \rightarrow 20^\circ$, then $20^\circ \rightarrow -20^\circ$, and concluding with $-20^\circ \rightarrow 0^\circ$ with no significant hysteresis observed. Stall is evidenced by the reduction in lift curve slope approaching $\delta = 14^\circ$. By $\delta = 20^\circ$ the flow over the airfoil flap is characterized by its separation envelope spanning the entirety of the flap length, as shown in Fig. 4. A free shear layer is revealed by the dye to be largely streamwise-oriented rather than adhering to the contour of the airfoil flap. The primary focus of the ensuing investigation is a deflection amplitude of $\delta_0 = 20^\circ$. This selection is intended to assess the efficacy of both the theoretical and empirical plunge-mitigation criteria in highly unsteady flows inviting of vortical dynamics.

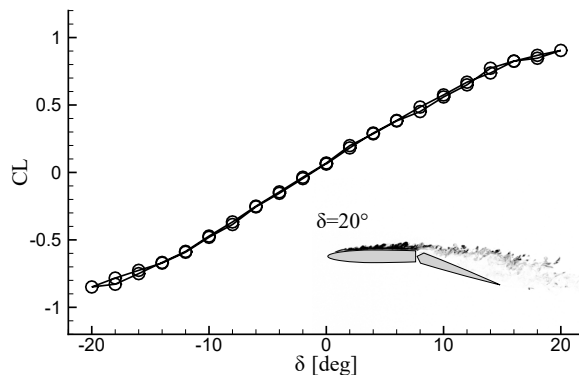


Figure 4. Static lift coefficient.

A. Theoretical Approach: Theodorsen's Model

The theoretical approach to harmonic plunge cancellation follows from enforcing a zero lift criterion of Theodorsen's model. Initial studies examined a deflection amplitude of $\delta_0 = 10^\circ$. As surmised from the static lift slope at $\delta = 10^\circ$ in Fig. 4, this deflection angle presents a nominally attached flow. When engaged in dynamic deflection, the rates of motion considered here are anticipated to support enhanced flow-attachment over the flap [1]. Note that from Eq. (10) the flap deflection phase lead is independent of airfoil plunge or flap deflection amplitudes, consistent with McGowan et al. [4]. However, there is a direct correlation between reduced frequency, k , and amplitude of plunge that may be theoretically canceled. An increase in reduced frequency of the flap actuation of the flap generates greater periodic lift, which in turn is capable of negating greater lift induced in airfoil plunge following more aggressive vertical acceleration profiles. The acceleration amplitude scales linearly with plunge amplitude. For this reason, reduced frequency

values of $k = [0.3989, 0.7979, 1.5959, 3.1919]$ were considered for a fixed flap deflection of $\delta_0 = 10^\circ$. The corresponding plunge amplitudes and deflection phase leads are summarized in Table 1.

As anticipated, with increasing k there was a decrease in plunge amplitude h/b , although greater non-circulatory forces were generated by the elevated acceleration profile in plunge. This trend is on display in the lift coefficient histories of Fig. 5. Direct force measurements were performed on the airfoil following three kinematic schedules: pure airfoil plunge ($\delta_0 = 0^\circ$), pure flap deflection ($h/b = 0$), and a combined plunge-deflection motion employing the predetermined deflection phase lead. An overarching feature among the pure plunge plots of Fig. 5 is the gradual phase shift of lift coefficient from nominally 90° out of phase from the plunge acceleration of $k = 0.39$ to the gradual synchronization of the lift history with the acceleration profile of $k = 3.19$, in agreement with phase plots of Theodorsen's model [13]. Pure deflection also experiences a gradual shift in lift history phase with increasing reduced frequency k . It should be noted that lift history plots for pure flap deflection are measured from experiment employing zero phase shift $\phi = 0^\circ$ in Eq. (1). Through application of the Theodrosen model, the pure deflection lift histories are of comparable magnitude to those of pure plunge. Pure deflection consistently produces slightly less lift than plunge and the minor disparity between the two histories' peak to peak lift is nearly doubled from $k = 0.39$ to $k = 3.19$. Nevertheless, when a flap deflection of $\delta_0 = 10^\circ$ was employed in conjunction with the theoretical plunge and phase values, there was a significant drop in lift among the four cases of Fig. 5. There are reductions in lift of 82.2%, 74.5%, 78.2%, and 87.2% from the pure plunge values for reduced frequencies of $k = 0.39, 0.79, 1.59,$ and 3.19 , respectively. The sizing and kinematic schedule of the flap is successful in enacting significant alleviation of lift generated by harmonic periodic vertical disturbance, congruent with the theoretical zero-lift enforcement of Eq. (5).

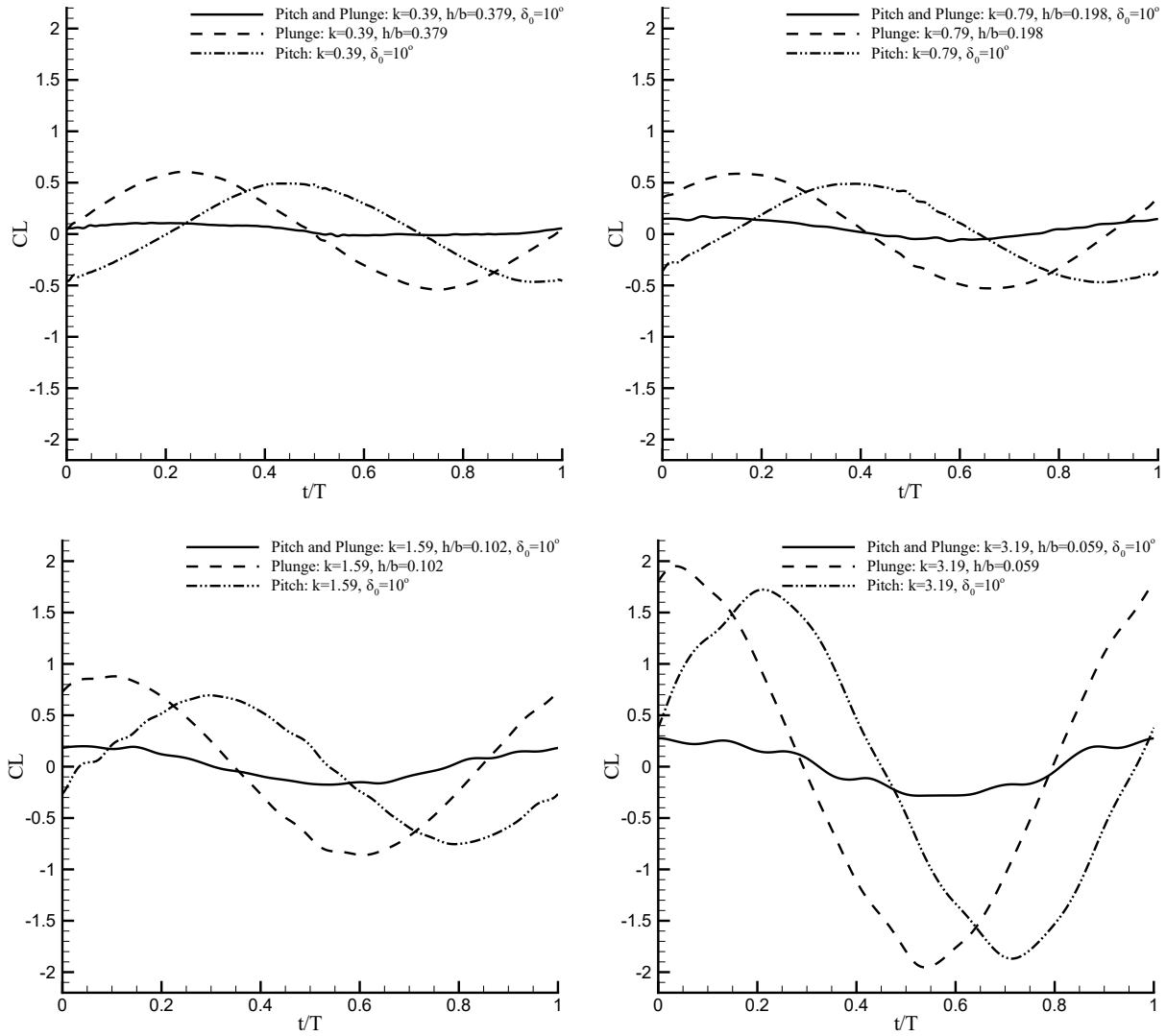


Figure 5. Theoretical plunge-deflection kinematics: lift history for $\delta_0 = 10^\circ$.

When the flap deflection amplitude was increased to $\delta_0 = 20^\circ$, it is expected that a larger plunge excursion could be canceled compared to the previously examined motions at the same reduced frequency for $\delta_0 = 10^\circ$. Lift coefficient histories for $\delta_0 = 20^\circ$ are presented in Fig. 6 for reduced frequencies $k = 0.79$ and 1.59 . For motion at $k = 0.79$, the plunge amplitude theorized for cancellation increased from $h/b = 0.1985$ for $\delta_0 = 10^\circ$ to $h/b = 0.3970$ for $\delta_0 = 20^\circ$. This motion resulted in an 82% reduction in lift from pure plunge. Likewise, for $k = 1.59$, plunge amplitude was increased to $h/b = 0.2050$, from which pure plunge lift was reduced by 81.4% by flap actuation. There is at present no obvious explanatory trend in cancellation, as at times the reduction in plunge-based lift by flap actuation bore greater success for the higher flap deflection amplitudes than for lower. This observation challenges intuition concluded from recourse to the small-angle, attached-flow theory of Theodorsen. Intuition is further confounded upon examination of the flow visualizations for $\delta_0 = 20^\circ$.

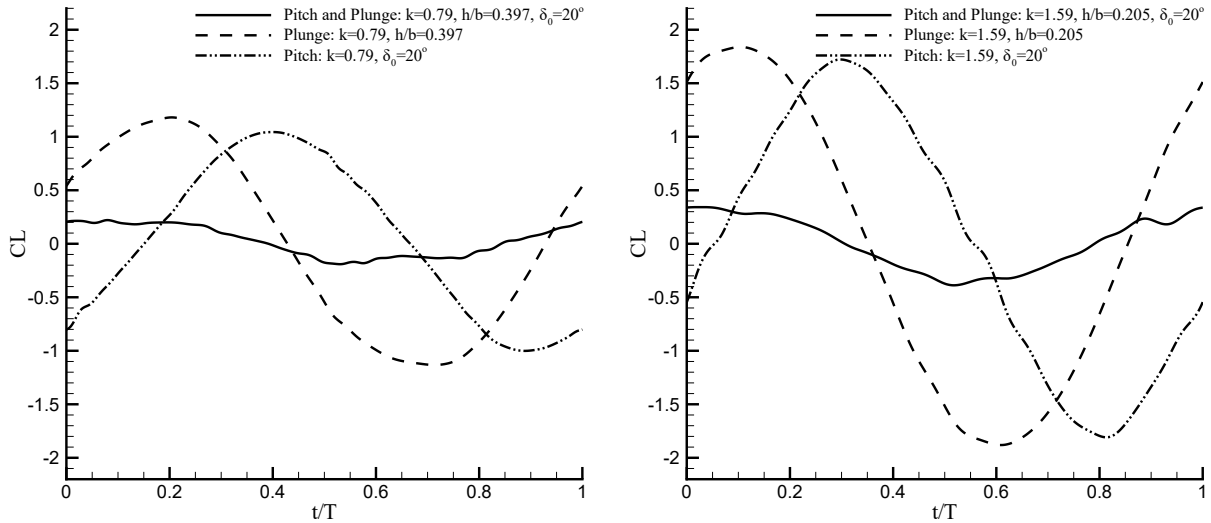


Figure 6. Theoretical plunge-deflection kinematics: lift history for $\delta_0 = 20^\circ$.

Fig. 7 catalogs the near-body flow field temporal evolution by way of select snapshots of dye visualization captured throughout a representative kinematic cycle for $k = 0.79$. In the case of pure plunge, leading-edge shear roll-up is prominently represented at $t/T = 0.25$. By $t/T = 0.5$ there is a strong eruption of dye-tagged vorticity emanating from the leading edge to produce a large leading-edge vortex. As the airfoil reciprocates in plunge at $t/T = 0.62$ the initial leading-edge vortex is detached and convected along the flap as it is encountered by the airfoil. The leading-edge shear layer on the upper surface of the airfoil ceases to exist, and what remains of the shear layer roll-up is detached from the leading edge and convected downstream. The illuminated surface of the airfoil now acts as the pressure surface and is devoid of vortical formations at $t/T = 0.88$. These unsteady leading-edge formations come as a result of the separation induced by fluctuations in effective angle of attack experienced in plunge. The temporal variation of effective angle of attack is shown in Fig. 9 where it is seen to peak at $\alpha_{\text{eff}} = 17.6^\circ$, well in excess of the stall angle.

Conversely, in pure flap deflection Fig. 7 reveals no vortical aberrations deviating from an otherwise attached flow along the leading edge and the fore element of the airfoil throughout the entire period. The flap deflection amplitude and rate do not appear to induce leading-edge transient formations. The effects of dynamic deflection appear to be isolated to the near-flap region. As the flap recedes from its maximum deflection at $t/T = 0.62$ the airfoil geometry causes a spurious shear layer mixing over the flap. The resulting formations, however, do not separate from the airfoil, but rather convect along the deflected flap. It would appear then, by inspection of flow visualization, that the onus of flap actuation is both the mitigation of added mass and the suppression of the leading-edge vortex associated with airfoil plunge. The third column of Fig. 7 shows the plunge-cancellation effects of flap actuation. By as early as $t/T = 0.25$ the flap's effect is discernible by inspection of the shear layer roll-up size which is reduced from that observed in pure plunge. Perhaps the most telling of leading-edge formation suppression comes at the end of the downstroke at $t/T = 0.5$ where the previous prominence of a leading-edge eruption of vorticity for pure plunge is now subdued in size and distribution for combined plunge and deflection. That is, the flap motion is not sufficient to provoke the outright cancellation of the leading-edge vortex formation but it does have substantial influence on its evolution. When the flap is engaged, the leading-edge phenomena appears more compact and in greater proximity to the airfoil surface. During the upstroke, the flap's deflection also appears to aid in the chordwise convection, and ejection, of vortical formations created in the previous downstroke, as observed at $t/T = 0.75$. Through these observations, the lift-canceling flow field does bear many of the hallmarks associated with the pure plunge flow field, suggesting the relation between force history and flow field history is complex.

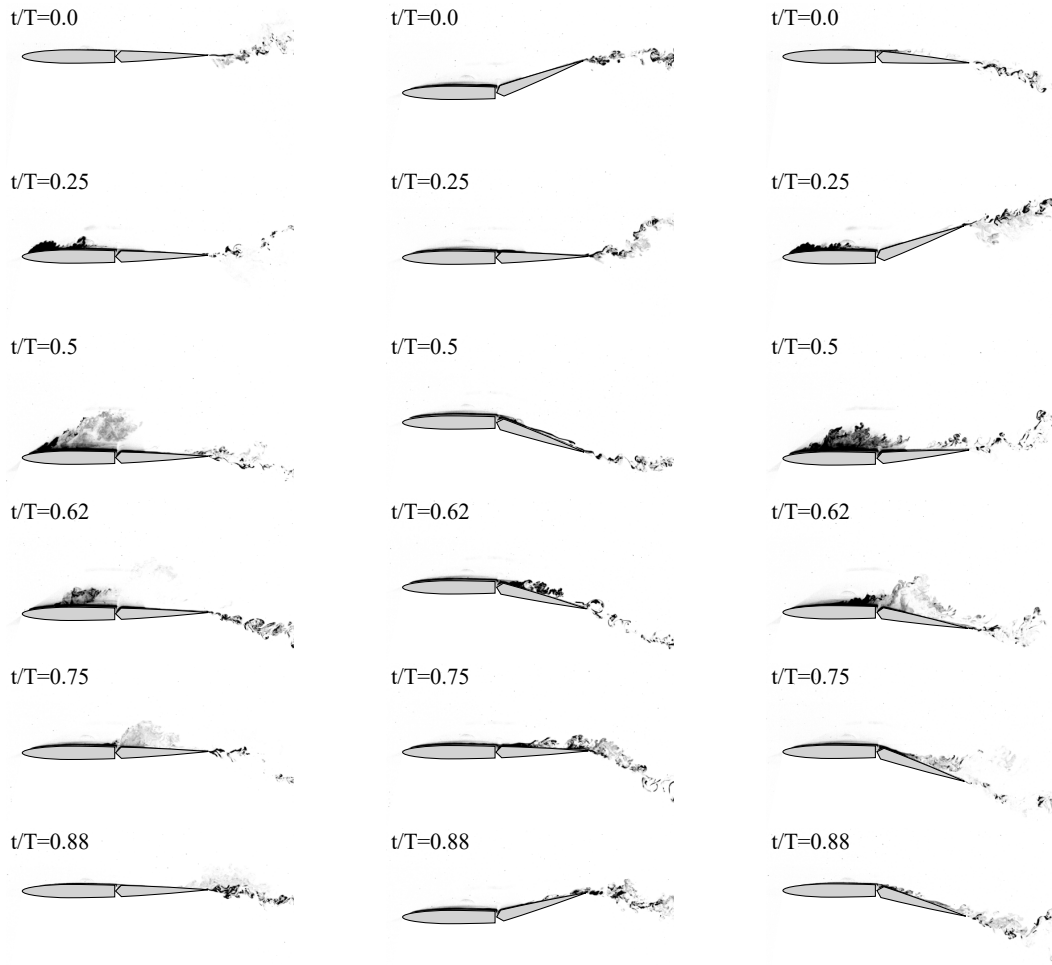


Figure 7. Theoretical plunge-deflection kinematics: flow field evolution over one period for $\delta_0 = 20^\circ$ at $k = 0.79$. Columns: (*left*) pure plunge, (*center*) pure deflection, (*right*) plunge and deflection.

In doubling the reduced frequency of motion to $k = 1.59$ the general flow field trend is the development of more coherent and compact structures. Fig. 8 catalogs the temporal evolution of the near-body flow field for $\delta_0 = 20^\circ$, corresponding to the theoretical plunge amplitude of $h/b = 0.205$ at $k = 1.59$ and an effective angle of attack peak of $\alpha_{\text{eff}} = 18.2^\circ$ (Fig. 9). For pure airfoil plunge, the semi-period of motion appears to approach the formation time of the leading-edge vortex. This is ascertained by the airfoil maintaining a concise concentration of vorticity in direct proximity to the leading edge by the completion of the downstroke at $t/T = 0.5$. This introduces an inherent latency in the convection of the leading-edge formation from that observed for $k = 0.79$ which translates to greater wake interactions during the subsequent upstroke at $t/T = 0.62$. By $t/T = 0.75$ the leading-edge vortex remains a rather prominent feature. Given this structure's prevalence throughout the plunge cycle it stands to reason its removal may prove desirable to realize mitigation or cancellation of plunge-based vertical disturbances. As previously observed in pure flap deflection, the leading edge bears no vortical formations induced by trailing-edge flap actuation, as demonstrated in Fig. 8. It is also apparent that flap actuation frequency preserves an attached flow over the flap for the duration of the flap cycle. Minor vortical elements convect along the chord induced by tripping of the boundary layer at the mid-chord joint. In combined airfoil plunge and flap deflection, vortical cancellation efforts prove quite effective. At $t/T = 0.5$ it appears the leading-edge vortex formation has been suppressed and what remains is the shear-feeding layer. During stroke reversal at $t/T = 0.62$ the wing is left with a semblance of a mixed boundary layer that is spread along the chord. Thus, at $k = 1.59$ the flow remains nominally attached for the entirety of the cancellation cycle.

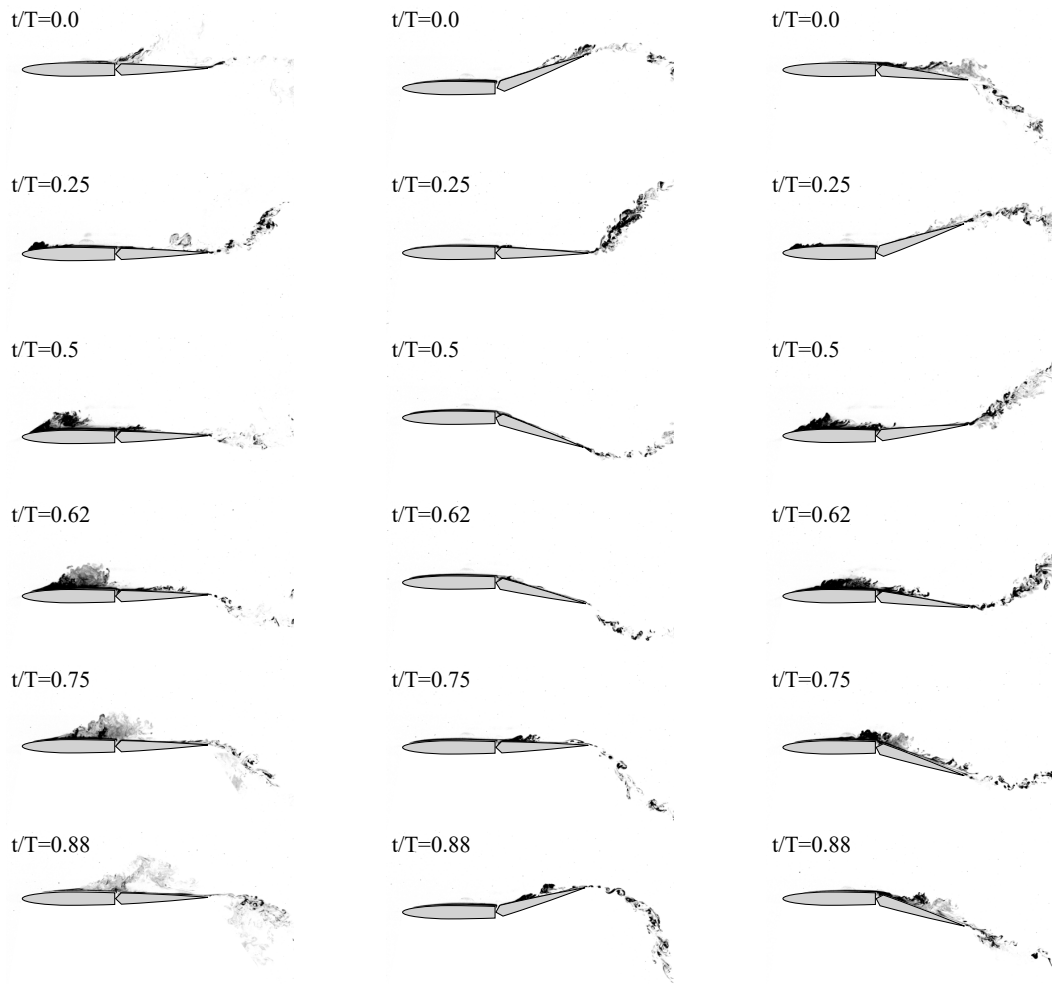


Figure 8. Theoretical plunge-deflection kinematics: flow field evolution over one period for $\delta_0 = 20^\circ$ at $k = 1.59$. Columns: (*left*) pure plunge, (*center*) pure deflection, (*right*) plunge and deflection.

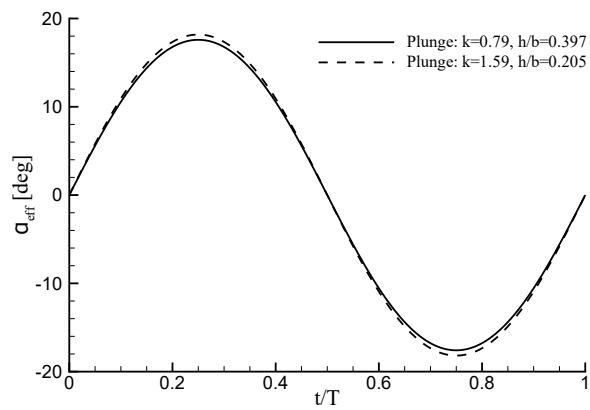


Figure 9. Effective angle of attack, α_{eff} , in plunge for theoretically-derived kinematics.

B. Empirical Approach: State-Space Model

Thus far, Theodorsen’s model has been applied to guide kinematic scheduling in plunge-cancellation efforts, and to astonishing success. In an attempt to improve the lift cancellation, a study exploring plunge mitigation via flap actuation with kinematic scheduling determined from empirical modeling of the lift response was explored. The desire here is to improve upon the cancellation efforts of the idealized Theodorsen model. For a flap deflection amplitude of $\delta_0 = 20^\circ$ at $k = 1.59$ Theodorsen’s model indicated a complementary plunge amplitude of $h_0/b = 0.2057$. The resulting lift measurements did leave room for improvement by way of further reducing the lift of combined plunge and deflection closer to zero. Thus it stands to reason that the appropriate plunge amplitude may be smaller than that provided by Theodorsen’s modeling given the lift surplus. To this end, the empirical model reveals a plunge amplitude of $h_0/b = 0.1565$ at $k = 1.59$ with $\delta_0 = 20^\circ$, a 23.9% reduction from Theodorsen’s model. This finding is in qualitative agreement with measured lift trends. The resulting lift histories of the empirically-derived kinematics are shown in Fig. 10, (left). In a departure from the theoretical modeling of Theodorsen, the peak to peak lift of pure plunge is now less than that of pure flap deflection. In motions of combined airfoil plunge and flap deflection, once again the resultant lift is significantly reduced from that produced in the pure plunge lift disturbance history. The empirical model boasts a 87.8% reduction from plunge-based lift, an overall improvement over the 81.4% reduction in the lift achieved using the theoretical modeling approach. Congruently, the reduced plunge amplitude of the empirical model is met with further suppression of leading-edge formations, as shown in Fig. 11. Even though the leading-edge roll-up in pure plunge is of smaller scale given the inherent decrease in plunge velocity due to the fixed reduced frequency, the cancellation efforts of combined plunge and deflection are apparent. Despite the reduction in plunge amplitude, the effective attack angle still manages a substantial peak of $\alpha_{\text{eff}} = 14^\circ$ (Fig. 12). In this instance, much of the plunge-induced formations are relegated to a thin layer of mixing at the end of the downstroke, $t/T = 0.5$ by the flap’s deflection. Beyond the halfstroke, boundary layer formations are expressly ejected into the wake by the reciprocating deflected airfoil.

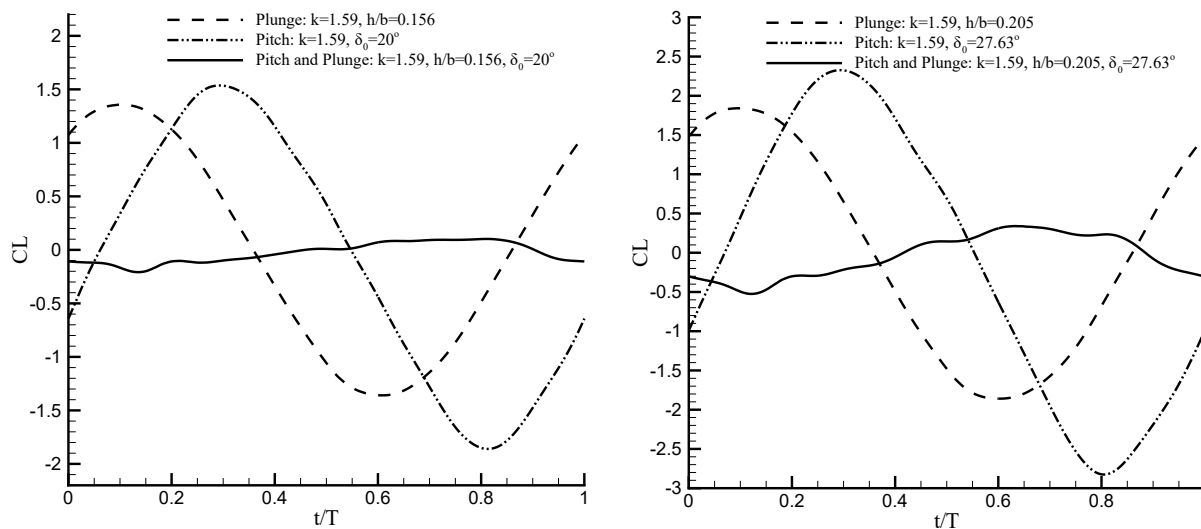


Figure 10. Empirical plunge-deflection kinematics: lift history for $k = 1.59$.

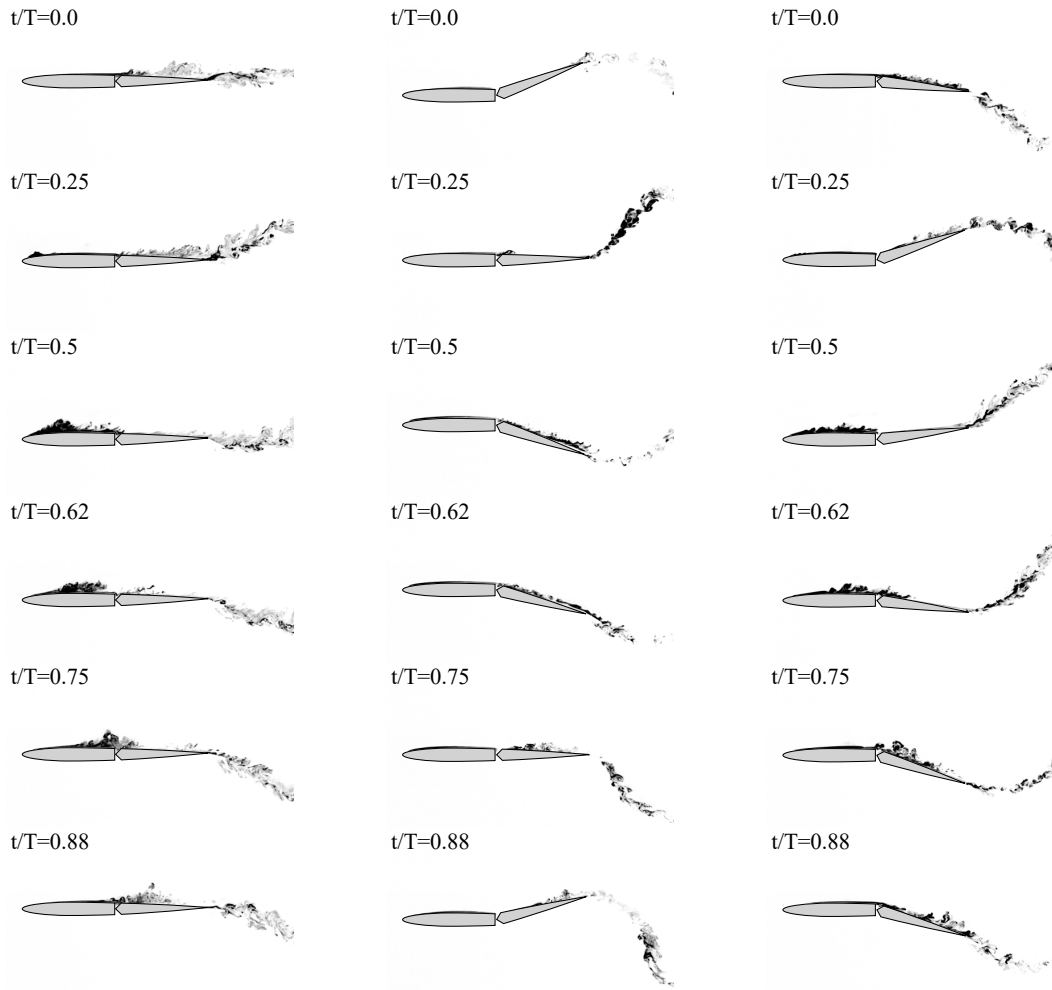


Figure 11. Empirical plunge-deflection kinematics: flow field evolution over one period for $\delta_0 = 20^\circ$ at $k = 1.59$. Columns: (*left*) pure plunge, (*center*) pure deflection, (*right*) plunge and deflection.

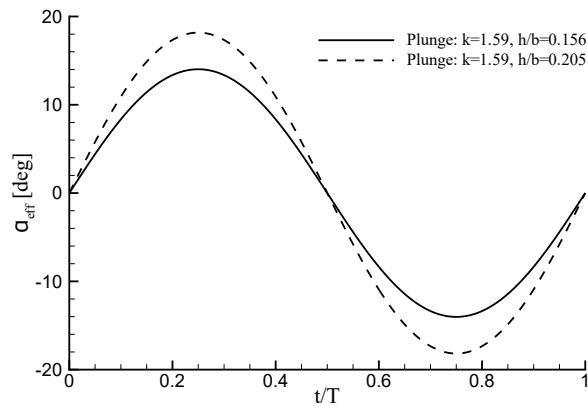


Figure 12. Effective angle of attack, α_{eff} , in plunge for empirically-derived kinematics.

As a final case for the empirical model, the plunge amplitude determined from Theodorsen's model for $\delta_0 = 20^\circ$ at $k = 1.59$ is employed as the input for the empirical model to determine a suitable flap deflection amplitude as output for cancellation. We retain the $h_0/b = 0.2057$ pure-plunge flow field of Fig. 8 (reproduced in Fig. 13) for its coherent leading-edge vortex, corresponding to a peak in effective attack angle

of $\alpha_{\text{eff}} = 18.2^\circ$ (Fig. 12). This case is intended to demonstrate that the gains in disturbance mitigation exhibited by the empirical model for $\delta_0 = 20^\circ$ at $k = 1.59$ are not merely the product of the reduced plunge amplitude but rather speak toward the efficacy of the empirical model. The pitch deflection amplitude determined using the empirical model is $\delta_0 = 27.63^\circ$. The corresponding lift histories are presented in Fig. 10, (right). With a phase lead of $\phi = 70.41^\circ$, the dynamics of the flap produce a 81.6% reduction of pure plunge lift. Upon examination of the flow field visualization in Fig. 13 we note the flow field remains attached in pure flap deflection motions for the duration of the kinematic cycle despite the greater deflection amplitude. In combined plunge and deflection motions, the resulting flow field is akin to the findings of the empirical $\delta = 20^\circ$ case in that there is outright suppression of the leading-edge vortex and an express ejection of the mixed boundary layer.

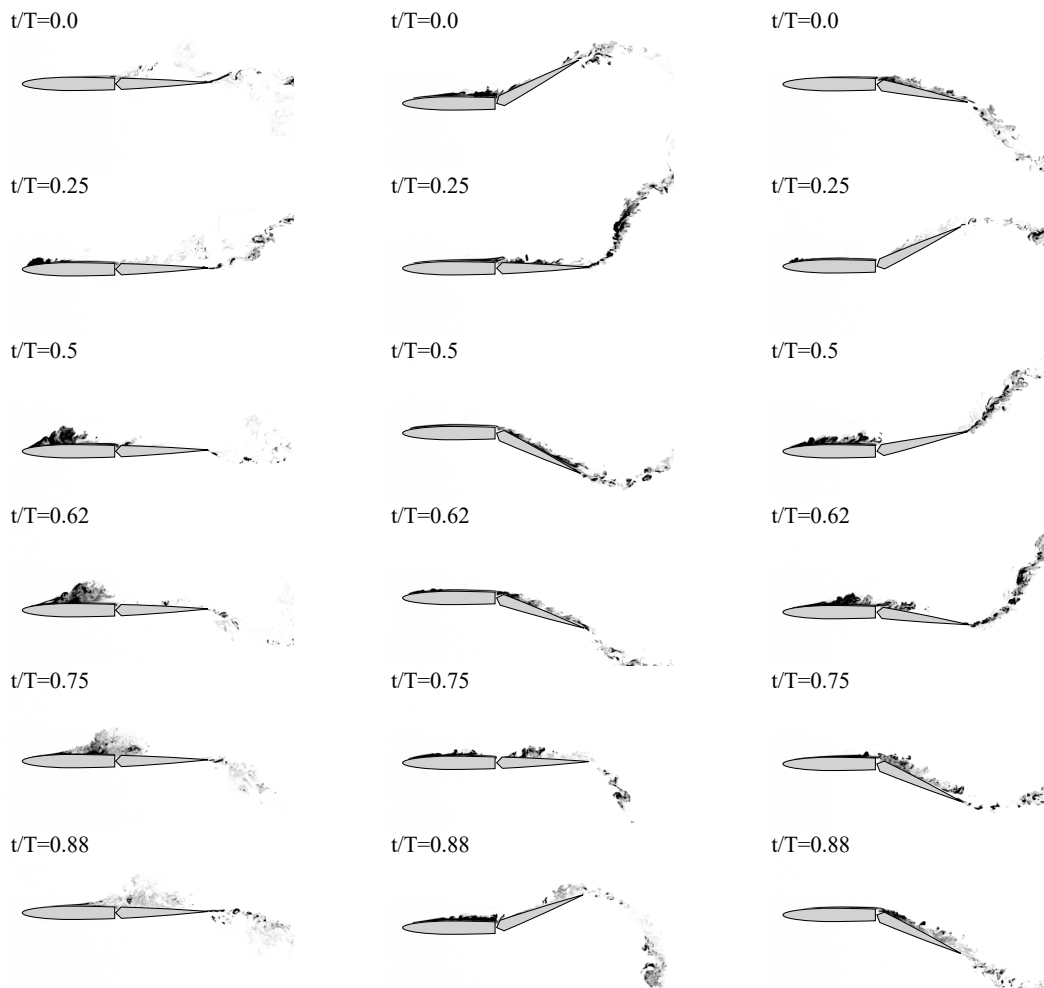


Figure 13. Empirical plunge-deflection kinematics: flow field evolution over one period for $\delta_0 = 27.63^\circ$ at $k = 1.59$. Columns: (left) pure plunge, (center) pure deflection, (right) plunge and deflection.

V. Conclusion

A conventional large-chord (50%) trailing-edge flap was deflected in periodic motions, with the fore-element of the airfoil at $\alpha_{\text{LE}} = 0^\circ$ fixed incidence, in the presence of an imposed “disturbance” instantiated as a sinusoidal vertical plunging motion of the whole airfoil. Using Theodorsen’s idealized attached-flow, small-angle approximation as a guide, flap deflection phase-lead and plunge amplitude were matched, for a given flap deflection amplitude and common frequency, such that the combined motion of airfoil plunge and flap deflection would give theoretical net cancellation of lift. Motions derived from Theodorsen’s model occurred over a time-period of from one to eight convective times, the latter approaching quasi-steady, and

the former dominated by added-mass and pitch-rate effects. Direct lift measurement in a water tunnel showed that full cancellation of lift was not achieved, even for small (10° amplitude) flap deflections; but for several amplitude-frequency combinations, the residual peak lift was only some 15% of the full (plunge-alone) lift. In an effort to improve upon the actuated flap's performance in canceling plunge-based lift, an empirical model was constructed to better inform the kinematic scheduling required for lift cancellation. In the empirical approach, separate models were constructed from pure airfoil plunge data and pure flap deflection data and linear superposition was employed to approximate the total force generated in combined plunge and deflection motions. Comparisons between the theoretical model and the empirical model were reserved for reduced frequencies $k = 1.59$ and flap deflection amplitudes $\delta_0 \geq 20^\circ$ to invite greater transient vortical formations. Lift histories revealed the performance of the empirical approach to be quite similar to the cancellation efforts of Theodorsen's model. Similarly, the resultant empirical phase-leads of flap deflection agree quite well with phase-lead values derived from Theodorsen's model. However, inspection of the accompanying flow visualization reveal greater suppression of the leading-edge vortex generated in pure plunge when employing the empirical models for cancellation.

References

- ¹ A. Medina, M.V. Ol, P. Mancini, and A.R. Jones. Revisiting conventional flaps at high deflection rate. *AIAA Journal*, 55(8):2676–2685, 2017.
- ² C.E. Brennen. A review of added mass and fluid inertial forces. In *Tech. Rep. CR 82.010, Naval Civil Engineering Laboratory*, Port Hueneme, CA 93043, 1982.
- ³ J.W. Jaworski. Thrust and aerodynamic forces from an oscillating leading edge flap. *AIAA Journal*, 50(12):2928–2931, 2012.
- ⁴ G.Z. McGowan, K. Granlund, M.V. Ol, A. Gopalarathnam, and J.R. Edwards. Investigation of lift-based pitch-plunge equivalence for airfoils at low reynolds numbers. *AIAA Journal*, 49(7):1511–1524, 2011.
- ⁵ W. Kerstens, J. Pfeiffer, D. Williams, and R. King. Closed-loop control of lift for longitudinal gust suppression at low reynolds numbers. *AIAA Journal*, 49(8):1721–1728, 2011.
- ⁶ D. Greenblatt and I.J. Wygnanski. The control of flow separation by periodic excitation. *Progress in Aerospace Sciences*, 36:487–545, 2000.
- ⁷ R.M. Rennie and E.J. Jumper. Experimental measurements of dynamic control surface effectiveness. *Journal of Aircraft*, 33(5):880–887, 1996.
- ⁸ R.M. Rennie and E.J. Jumper. A case for pseudo-steady aerodynamic behavior at hgh motion rates. In *35th Aerospace Sciences Meeting and Exhibit*, pages 97–0617, Reno, NV, 1997.
- ⁹ T. Albrecht, T. Weier, G. Gerbeth, B. Monnier, and D. Williams. Separated flow response to single pulse actuation. *AIAA Journal*, 53:190–199, 2015.
- ¹⁰ Karl Johan Åström and Björn Wittenmark. *Computer-Controlled Systems: Theory and Design*. Prentice-Hall, 1997.
- ¹¹ S.T.M. Dawson M.S. Hemati and C.W. Rowley. Parameter-varying aerodynamics models for aggressive pitching-response prediction. *AIAA Journal*, 55(3), 2017.
- ¹² Peter Van Overschee and Bart De Moor. *Subspace Identification for Linear Systems: Theory, Implementation, Applications*. Kluwer Academic Publishers, Boston, 1996.
- ¹³ S. L. Brunton and C. W. Rowley. Empirical state-space representations for theodorsen's lift model. *Journal of Fluids and Structures*, 38:174–186, 2013.